Remote Detection of Weapons of Mass Destruction using Wideband Radar

Ershad Sharifahmadian
University of Houston, Clear Lake

Yoonsuk Choi,
California State University, Fullerton

Shahram Latifi
University of Nevada, Las Vegas

ABSTRACT
Gamma and neutron detection are typical methods used for detection of Weapons of Mass Destruction (WMD). However, radiation related to gamma-rays can be easily shielded. Moreover, environmental conditions affect the efficiency of current methods for detection of fissile materials, and also reduce the range of detection. Here, a wideband target recognition method is proposed with the ability to detect a target− in particular the WMD− from a distance and identify the type of the target. As wideband data includes a broad range of frequencies, it can reveal information about both the surface of the target and its content. At first, the presence of the target and its location are estimated. Then, the estimated target is recognized by evaluating collected wideband data with information from wideband signature library which has already been built. Based on the experimental results, it is concluded that the proposed technique can be a promising approach for standoff target detection. As an example, the approach could identify the stainless steel sheet as the target with the best accuracy of 74%. Although the proposed method is designed for WMD detection, it can be extended to any application of target detection.

General Terms
Remote sensing

Keywords
Return loss, Target recognition, Wideband radar, WMD detection, Wavelet transform.

1. INTRODUCTION

1.1 WMD Detection
Every country requires to enhance its ability to deal with a potential threat from terrorism involving the smuggling of nuclear weapons, or materials to make them into the country. It is suggested that any type of transportation (e.g. cargo ships and trucks) at entry ports need to be closely monitored. To secure entry ports, new monitoring technologies are required to rapidly identify a wide range of threats and suspicious materials without interrupting the flow of trade administration or changing the existing cargo supply chain [1]-[4]. Whereas radiation related to gamma-rays, X-rays, and α particles can be simply shielded, identification of spontaneous fission neutrons has been studied [5], [6]. Nonetheless, current techniques to detect fissile material by sensing gamma rays or neutrons have limited distance of effectiveness, due to environmental conditions [7].

1.2 Wideband Technology
Unlike typical narrowband radar system, the WideBand (WB) radar spreads electromagnetic waves across a wide range of frequencies [8].

WB waves can be utilized in such applications as range measurement [9], or object recognition. In geophysical surveying, wideband radar system has been utilized to find ice thickness, or analyze the rock construction. Because of the wideband nature of the WB signal, the WB signal can pass through ice and various solid materials with different penetration degrees. In fact, electromagnetic waves are reflected by any unforeseen variation in the index of refraction, which is why the wideband waves are capable of providing subsurface or underground information [10]. Wideband technology was originally used for military applications due to their ability to detect targets among trees and under the ground. Most research has been done to improve detection accuracy over longer range. The wideband radar system was mainly developed after the development of solid state devices to provide high-power wideband waves [11].

Due to the ability of short-duration impulses to collect information about concealed objects, there have been many studies to create remote detection system based on WB technology [12].

The wideband radar detection techniques have been developed for foliage penetration, mine detection, and high-resolution mapping. Foliage can hide vehicles, instruments, structures from airborne observers [13].

Because of the presence of low frequency components in WB radar waves, penetration of most dielectric materials is assured enabling through-wall target recognition, with good ability to penetrate such building materials as wood, concrete, and brick. Furthermore, WB target detection can be run in dust-filled environments, where infrared and optical sensors fail [10], [14], [15]. Hyperspectral, ultrasound and infrared sensors collect surface information about objects in a scene [16]-[20]. But, penetration through such denser objects as fiberglass, wood, brick and concrete requires frequency ranges less than 10 GHz [21].

To generally penetrate into an object and collect information about its content, it is required that parameters relating to wideband radar signals be set exactly. These parameters are bandwidth, radiated power, center frequency, pulse repetition frequency, polarization, etc.

1.3 Return Loss
The Return loss is a measure of the reduction in electric and/or magnetic field strength from reflection caused by a material. Return Loss (RL) is formulated as follows [10], [22]:

$$R.L = 10log_{10}(\frac{Incident\ Power\ Density}{Reflected\ Power\ Density}) \quad (1)$$

In next section, the proposed target recognition method is explained. The results of experiments are presented in section

3. Section 4 concludes the paper.

2. TARGET RECOGNITION

The WB-based target recognition is based on the fact that electromagnetic waves penetrate through different materials at different rates. While high-frequency waves have a higher rate of absorption by materials, low-frequency waves can pass through materials more easily, making the object recognition simpler.

The block diagram of the proposed WB-based target recognition method is shown in the figure 1.

The transmitter antenna sends wideband signals toward a target in a scene. When electromagnetic waves pass through a material, the power of the WB waves will be subject to a certain level of attenuation relating to characteristics of the material. At receiver side, based on received wideband waves from the scene, the target can be recognized.

Using the proposed technique, first, the presence of the target and its location are estimated. Then, the target is recognized using evaluation of target's return loss with information in a wideband signature library.

The WB signature library includes the value of conductivity, permeability, permittivity, return loss at different frequencies for possible materials related to specific targets, in particular WMD.

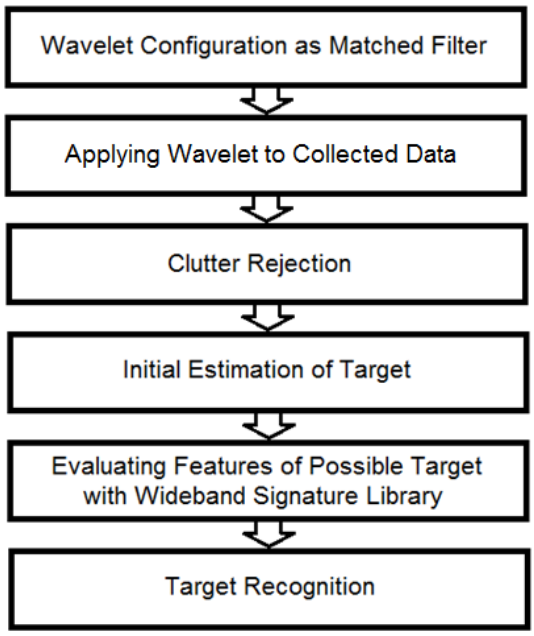

Figure 1. Block diagram of the WB-based target recognition method

2.1 Wavelet Analysis

The wavelet transform presents suitable localization in both frequency and time domains. It provides low frequency resolution and high time resolution at high frequency, and high frequency resolution and low time resolution at low frequency.

The wavelet transform contains the wavelet coefficients of the expansion of the input signal corresponding to a basis $f_{a,\tau}(t)$, and every value of $f_{a,\tau}(t)$ is a translated and dilated form of the mother wavelet, $f(t)$. The basis function is formulated as follows [10]:

$$f_{a,\tau}(t) = \frac{1}{\sqrt{|a|}} f\left(\frac{t-\tau}{a}\right) \quad (2)$$

where a is the scale of the wavelet. The wavelet coefficients represents the input signal $x(t)$, and those coefficients are calculated as:

$$W_x(a,\tau) = \frac{1}{\sqrt{|a|}} \int x(t) f^*\left(\frac{t-\tau}{a}\right) dt \quad (3)$$

To enhance the signal-to-noise-ratio in the narrowband radar detection, a matched filter is typically proposed. The matched filter is defined as:

$$y(t) = \int_{-\infty}^{+\infty} i(k) g(t-k) dt \quad (4)$$

where $g(t)$ is the template of received WB signals from a target, $i(t)$ *is* the collected WB signals by receiver antenna, and $y(t)$ is the output of the matched filter.

It is assumed that the value of a is constant. By looking at the equation (3) and (4), it is concluded that those equations are similar. In other words, the wavelet transform acts as the process of matched filtering. Before applying the wavelet transform to input data, it is required to match the scale of the wavelet transform to the frequency of the collected wideband signals. Thus, the scale a corresponding to F_a —the frequency of the received wideband signals— is defined as follows [10], [23], [24]:

$$a = \frac{F_0}{F_a \cdot \Delta} \quad (5)$$

Where Δ is the sampling period, and F_0 is the center frequency of the mother wavelet.

After the obtaining the wavelet' scales –During experiments, the center frequency of the WB signals change, so it is necessary to calculate the wavelet's scale for each center frequency– the wavelet transform is applied to collected wideband data. Then, the envelope of wavelet output is calculated. Afterwards, the clutter rejection followed by a thresholding is utilized.

During the clutter rejection, the every received wideband signal from a target in a scene is separated from reflected signals from antenna coupling and the scene without the presence of the target.

Up to this point, the presence of the target and its location are estimated.

2.2 Return Loss Calculation

After estimating the presence of the target, the values of return loss at different center frequencies—frequencies set for radiated wideband signals— are calculated to recognize the target in the scene. Next, the values of calculated return loss correspond to each material in the scene are compared with the values of return loss from the wideband signature library.

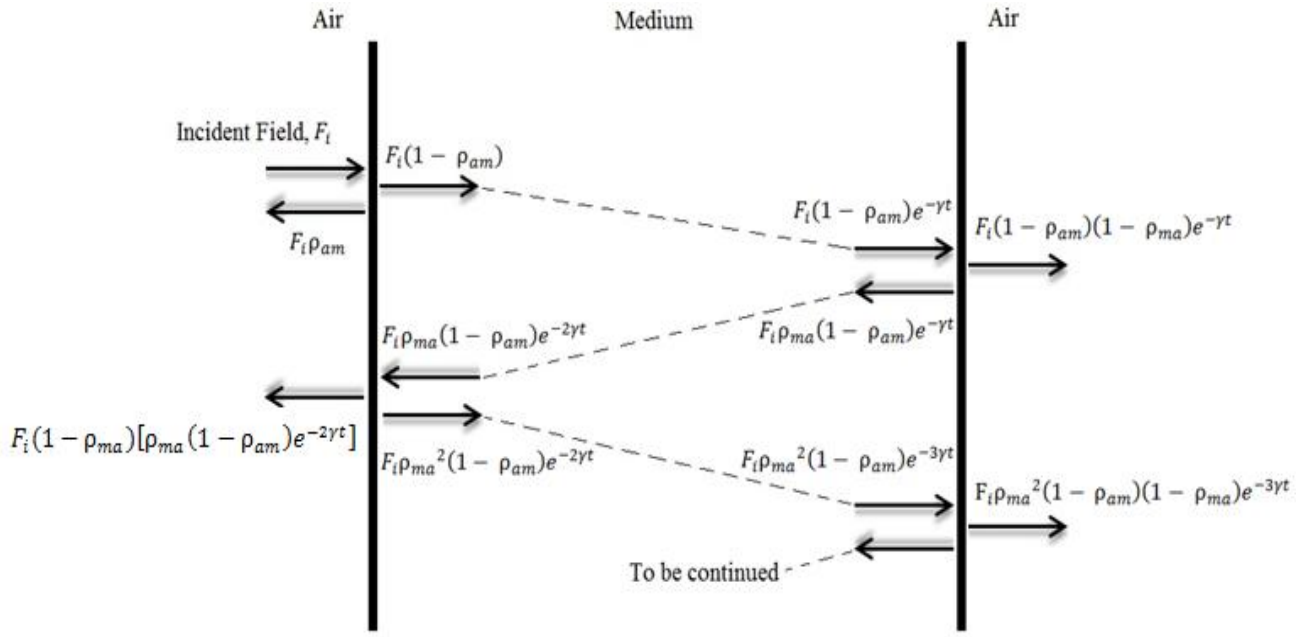

Figure 2. Reflection and transmission caused by a flat material [25]

The proposed method can identify the target in the scene based on how much the values of calculated return loss and the values of return loss from the wideband signature library are similar together. As comparison is done for the values of return loss at various center frequencies, the possibility of false identification is dropped.

2.3 Target Identification

In this section, the relation between electromagnetic characteristics of a material with its return loss is shown, and it is demonstrated how electromagnetic features of materials are used to identify a target.

To identify a specific target (e.g. WMD) using the proposed method, first, different materials related to that target are categorized based on their electromagnetic characteristics. Then, their electromagnetic characteristics are utilized during comparison of calculated RL's– RL's from a scene– with RL's from the wideband signature library.

Every material can be defined as a layer with a certain thickness (Figure 2). Based on the figure 2, the ratio of the reflected field to the incident field is formulated as follows [25]:

$$\frac{F_R}{F_i} = \rho_{am} + e^{-2\gamma\cdot t}\rho_{ma}(1-\rho_{am})(1-\rho_{ma})(1-\rho_{ma}^2 e^{-2\gamma\cdot t})^{-1} \quad (6)$$

where $\rho_{ma} = \frac{K-1}{K+1}$ is the reflection coefficient at the medium-to-air interface, $\rho_{am} = \frac{1-K}{1+K}$ is the reflection coefficient at the air-to-medium interface, $\gamma = \alpha + j\beta = \sqrt{j\omega\mu(\sigma + j\omega\varepsilon)}$ is the propagation constant, and F_R and F_i are the reflected field and incident field, respectively.

$$K = \frac{Z_w}{Z_m} = \frac{q\sqrt{\mu_0/\varepsilon_0}}{\sqrt{j\omega\mu/\sigma+j\omega\varepsilon}} \quad (7)$$

where Z_m is medium impedance, and Z_w is wave impedance in free space, σ is the conductivity of a material [S/m], μ is the permeability, μ_0 is the absolute permeability of the air, q=1 for far field, and $\varepsilon_0 = 8.854 \times 10^{-12}$ is the absolute permittivity of air. More information on how to obtain $\frac{F_R}{F_i}$ is available on [25].

The relation between the power density and electromagnetic field is defined as follows [25]:

$$\frac{P_R}{P_i} = \frac{S_R}{S_i} = \left(\frac{F_R}{F_i}\right)^2 \quad (8)$$

Therefore, the return loss for the flat layer of a material is defined as:

$$\text{R.L} = 20\log_{10}\left(\frac{1}{\left|\frac{1-K}{1+K} + e^{-2\gamma\cdot t}\left(\frac{K-1}{K+1}\right)\left(\frac{2K}{K+1}\right)\left(\frac{2}{K+1}\right)[1-(\frac{K-1}{K+1})^2 e^{-2\gamma\cdot t}]^{-1}\right|}\right) \quad (9)$$

when $\phi \neq 0$ (the angle of incident electromagnetic wave with the flat layer), the reflection coefficient, (e.g. ρ_{am}), can be written based on Fresnel reflection coefficient as [26], [27]:

$$\Gamma_{s,h}^m = \frac{1-e^{-j2\tau\cdot t}}{1-\Gamma_{s,h}^2 e^{-j2\tau\cdot t}}\Gamma_{s,h} \quad (10)$$

where $\Gamma_{s,h} = \frac{2\pi}{\lambda}\sqrt{\left(\varepsilon_r - \frac{j\sigma}{\omega\varepsilon_0}\right) - sin^2(\phi)}$, is the Fresnel reflection coefficient for the half-plane waves for the perpendicular and parallel polarization.

It is seen that return loss generally depends on the frequency of radiated radar signals, and electromagnetic features– conductivity, permeability, permeability– of the medium as reflector.

To identify specific targets in a scene–it is assumed that background data is already available in the scene– it is possible to build a comprehensive signature library with conductivity, permeability, and permittivity, return loss of materials related to the specific targets under different frequencies and environmental conditions (e.g. temperature). In fact, the reference information– information includes reference return loss, conductivity, permeability, and permittivity– from the signature library is utilized for target recognition.

When the reflectivity of a material increases, its RL decreases (i.e. $F_R \uparrow$ and RL $\downarrow$).

During WB data collection, the radiated power from transmitter antenna gradually increases to better discriminate targets. In fact, targets with low reflectivity cannot be detected at low radiated powers. In other words, dielectric materials with $\sigma \approx 0$ will be better sensed at high power radiated signals.

Moreover, the center frequency of WB signals gradually changes during WB data collection to better discriminate targets. As the frequency increases, the relative permeability drops. Therefore, a significant change will be seen in reflectivity of materials with high conductivity and relative permeability. As an example, relative permeability for Iron ($\sigma_r = 0.17$) equals 600@3MHz, 500@10MHz, and 50@ 1GHz [28]. Comparing with Copper ($\sigma_r = 1, \mu_r = 1$) , the reflectivity of Iron significantly increases at GHz frequency range. But, reflectivity of Copper does not significantly change in the frequency range from MHz to GHz.

The conductivity is the intrinsic property of a material. For materials that their conductivity is not zero (e.g. metals), when conductivity changes, the reflectivity changes. For example, at frequency range of GHz, metals with high conductivity show stronger reflections compared with metals with low conductivity; relative permeability of most metals is similar at frequency range above 1 GHz (i.e. $\mu_r \approx 1$), and does not affect their reflectivity. Thus, conductivity plays an important role.

Furthermore, the relative permittivity of most materials decreases with increasing frequency (MHz to GHz), and reflectivity of materials, in particular dielectric materials, changes. As an example, a fiberboard ($\mu_r \approx 1$) with the moisture content of 8% has the resistivity–that is the inverse of conductivity– of 3×10^5, and its relative permittivity decreases with increasing frequency (ε_r =1.175 @600MHz, 1.16 @700MHz, 1.15 @800MHz, 1.13 @900MHz, 1.125 @1GHz). A fiberboard with the moisture content of 0% (i.e. oven-dried fiberboard) has the resistivity of 10^{16} and $\varepsilon_r = 1$ [29]. It ought to be noted the angle of incidence with a target surface, and polarization of radar signals affect reflections from materials in a scene.

In conclusion, several classes (e.g. metals, woods, etc.) and subclasses (e.g. metals with high conductivity) have been defined based on electromagnetic characteristics of materials in proposed method. During the process of RL comparison, the support vector machines are utilized to better classify the calculated RL data.

3. RESULTS

During the experiments, the Impulse Radiating Antenna (IRA-3Q) is utilized [30], and different types of metal sheets are chosen as targets. Here, the results about the Stainless Steel sheet, and the ASTM B370 Copper sheet are presented. The stainless steel includes 90% Iron, 10% other materials. ASTM B370 Copper includes more than 99% Copper, and less than 1% other materials. The initial distance between IRA-3Q and the sheets is 9 feet, and sheets are close to each other. Then, the distance between IRA-3Q and the sheets changes to 10, 11, 12, 13 feet. 20 experiments are done for each distance, and each experiment takes 10 seconds.

At the beginning of experiments, it is assumed that sheets are unknown, and the target of interest is stainless Steel. The WB signals is radiated toward the sheets, then reflected WB signals are collected. The center frequency of signals changes from 600-1000MHz. First, objects in the scene –Stainless Steel, Copper, sheet holders, tripods– are detected and discriminated. Then, the identification process is performed.

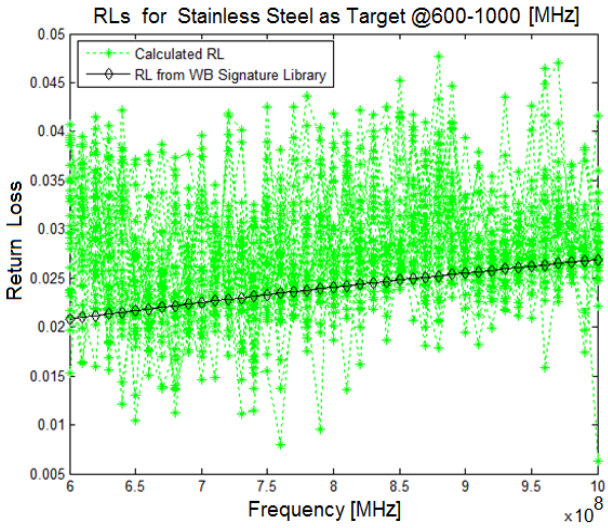

Figure 3. Calculated RL's and RL values from the WB signature library for the stainless Steel sheet

After WB data collection, the wavelet transform is applied to collected WB signals. The Symlet 16 wavelet is selected as the mother wavelet– Symlet 16 is chosen because its shape is similar to radiated WB signals – and applied to the collected WB signals. The output of applying the Symlet 16 wavelet is considered as the output of the WB matched filter. After the clutter rejection, the location of the target is estimated. In all experiments, the distance to targets was estimated, and the ranging error was less than 15 inches.

After estimating the presence of targets, the values of return loss are calculated at the selected frequencies.

Based on how close the calculated RL data are to their respective values in the WB signature library, the type of target can be identified. Figure 3 shows the calculated RL's –those are calculated based on reflections from steel surface– follow the variation of the RL's for the stainless steel (σ_r =0.02) from the wideband signature library at selected frequencies (600MHz to 1GHz). Eventually, the stainless steel is recognized with the identification rate of ~ 74%. The Identification Rate (IR) is defined as

$$\frac{Number\ of\ correct\ identification\ for\ target\ of\ interest\ in\ all\ experiments}{Total\ number\ of\ Experiments}.$$

As mentioned before, metals with high relative conductivity show stronger reflections compared with metals with lower σ_r.

As seen in figure 3 and figure 4, Copper (σ_r =1) has stronger reflections compared with stainless Steel (σ_r =0.02). In fact, for higher σ_r@ 600MHz-1GHz, F_R is higher, then RL is lower.

Although the MHz frequency range is used, however, when the wavelength of radar signals is almost twice the target size (e.g. 600MHz signals has λ=1.639 feet), a half-wave resonance effect can produce a significant reflection.

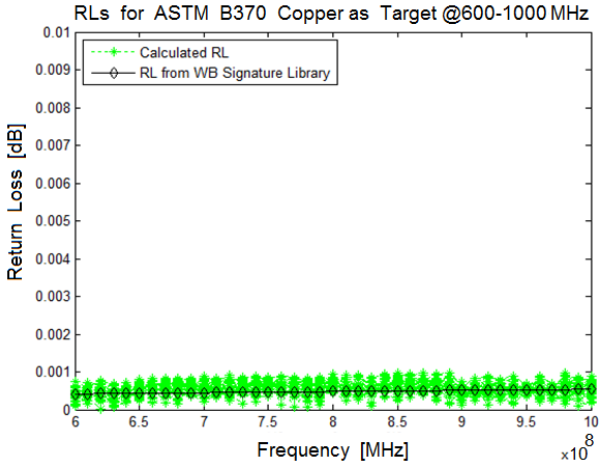

Figure 4. Calculated RL's and RL values from the WB signature library for the ASTM B370 Copper sheet

4. CONCLUSION

In this paper, a wideband radar target recognition method was proposed to detect a target and recognize its type. Originally, the method was proposed for WMD detection as the WB signature library includes materials related to the WMD packing or handling (e.g. Beryllium). However, the approach can be extended to other applications of remote sensing and target detection. The proposed WB-based method can reveal information about target's surface and content. To improve the initial target detection and to better track variable center frequencies—center frequencies of the radiated WB signals change during experiments— the collected WB data is processed in the wavelet domain. During the experiments, the presence and location of targets were estimated. Then, it was attempted to identify targets based on the WB data collected at different center frequencies and different radiated powers. As an example, the stainless steel was identified with the best accuracy of 74%.

Environmental conditions, thermal noise, electromagnetic interference from other RF sources such as cellphone signals have negative impacts on the procedure of target recognition. But, these are common problems for all target detection methods. However, by appropriately setting parameters of radiated signals, and building a comprehensive signature library including reference information under different frequencies and environmental conditions (e.g. temperature), it is possible to identify the type of targets from a distance.

Detecting shielded fissile materials is very difficult. For example, Gamma detectors cannot detect WMD shielded by Lead. However, it is possible to detect the shield (i.e. lead) using the proposed approach, and estimate there could be something behind the shield. For future work, the impact of radioactive radiation on the frequency content of reflected WB signals will be studied and evaluated.

5. ACKNOWLEDGEMENT

Authors would like to thank Prof. Robert Schill from the department of electrical and computer engineering, UNLV, for his supports. This work was supported (in part) by the Defense Threat Reduction Agency (DTRA), basic research award # HDTRA1-12-1-0033, and the National Science Foundation (NSF) award #EPS-IIA-1301726. Any findings expressed in the material are those of the authors and do not necessarily reflect the views of DTRA or NSF.

6. REFERENCES

[1] Rudzinski, C., et. Al, 2010, "Screening maritime shipping containers for WMD," IEEE Inter. Conf. on Technologies for Homeland Security (HST), 2010, pp.460-466.

[2] Mahin, D. A., "Addressing the threat: An examination of science and technology policy addressing weapons of mass destruction," IEEE Inter. Symp. on Technology and Society, 2006, pp.1-12.

[3] Archambault, B., et.al, "Transformational Nuclear Sensors-Real-Time Monitoring of WMDs, Risk Assessment & Response," IEEE Inter. Conf. on Technologies for Homeland Security, 2010, pp.421-427.

[4] Young, K. L., "WMD Technology Evaluation and Training Range," IEEE Inter. Conf. on Technologies for Homeland Security, 2009, pp.591-598.

[5] Athanasiades, A., et.al, "High Sensitivity Portable Neutron Detector for Fissile Materials Detection," IEEE Nuclear Science Symp., 2005, pp.1009-1013.

[6] Benettoni, M., et. al "Muon radiography with the CMS Muon Barrel chambers," IEEE Nuclear Science Symposium, 2007, pp.1021-1025.

[7] Ziock, K. P., et. al, "Large Area Imaging Detector for Long-Range, Passive Detection of Fissile Material," IEEE Trans. on Nuclear Science, Vol.51, No.5, 2004, pp. 2238-2244.

[8] Taylor, J. D., [Ultra-wideband radar technology,] CRC press; 1st edition, 2000.

[9] Sharifahmadian, E., and Ahmadian, A., "Adaptive signal processing algorithm for remote detection of heart rate (HR) using ultra-wideband waveforms based on principal component analysis," 31st IEEE EMBS Annual Inter. Conference, 2009, pp.5717–5720.

[10] Sharifahmadian, E., Choi, Y., and Latifi, S., "Wavelet-based Identification of Objects from a Distance" SPIE International Conference on Signal Processing, Sensor/Information Fusion, and Target Recognition XXIII, Vol.9191, USA, 2014, pp.1B1—1B8.

[11] Cramer, J. M., Scholtz, R. A., and Win, M. Z., "On the analysis of UWB communication channels", IEEE Military Communications Conference, vol. 2, 1999, pp.1191-1195.

[12] Sharifahmadian, E., Choi, Y., and Latifi, S., "Remotely detecting weapons of mass destruction," SPIE Newsroom, DOI: 10.1117/2.1201308.005057, 2013.

[13] Davis, M. E., "Developments in foliage penetration radar," International Radar Conference- Surveillance for a Safer World, 2009, pp.1-6.

[14] Slimane, Z., et. al, "OFDM based UWB synthetic aperture through-wall imaging radar," 3rd Inter. Conf. on Broadband Commu., Information Technology and Biomedical Applications, 2008, pp. 293-300.

[15] Salman, R., and Willms, I., "A novel UWB radar super-resolution object recognition approach for complex edged objects," IEEE ICUWB, 2010, pp.1-4.

[16] Lubecke, V. M., et. al, "Through-the-wall radar life detection and monitoring," IEEE Microwave Symposium, 2007, pp.769-772.

[17] Choi, Y., et.al, "Quality Assessment of Image Fusion Methods in Transform Domain", International Journal on Information Theory, Vol.3, No.1, Jan. 2014, pp.7—18.

[18] Sharifahmadian, E., and Latifi, S., "Advanced hyperspectral remote sensing for target detection" IEEE International Conference on Systems Engineering (ICSEng), 2011, pp.200-205.

[19] Marsousi, M., et.al, "Fast and automatic LV mass calculation from echocardiographic images via B-spline snake model and markov random fields," Annual International Conf. IEEE EMBS, 2009, pp.3633-3636.

[20] Lin, M., Zhongzhao, Z., and Xuezhi, T., "A novel through-wall imaging method using ultra-wideband pulse system," IEEE Conference on Intelligent Hiding & Multimedia Signal, 2006, pp.147-150.

[21] Braga, A. J., and Gentile, C., "An ultra-wideband radar system for through-the-wall imaging using a mobile robot, IEEE Conference on Communications, 2009, pp.1-6.

[22] Tsaliovich, A., [Electromagnetic shielding handbook for wired and wireless EMC applications,] Kluwer Academic Publishers, 1999.

[23] Abry, P., Goncalves, P., Vehel, J. L., [Scaling, Fractals and Wavelets], Wiley-ISTE; 1st edition, 2009.

[24] Jenkins, R. L., Dewberry, B., and Joiner, L., "Wavelet Analysis of Impulse Ultra-Wideband Radar", Proc. of the IEEE SoutheastCon, 2010, pp.155–158.

[25] Sharifahmadian, E., Choi, Y., and Latifi, S., "A Simulation Study of Detection of Weapon of Mass Destruction based on Radar" SPIE International Conference on Chemical, Biological, Radiological, Nuclear, and Explosives (CBRNE) Sensing XIV, Vol. 8710, USA, 2013, pp. Y1—Y12.

[26] Sato, K., et. al, "Measurements of reflection characteristics and refractive indices of interior construction materials in millimeter-wave bands," 45th IEEE Vehicular Technology Conference., vol. 1, July 1995, pp. 449–453.

[27] Karousos, A., Koutitas, G., and Tzaras, C., "Transmission and Reflection Coefficients in Time-Domain for a Dielectric Slab for UWB Signals," IEEE Vehicular Technology Conference, May 2008, pp.455—458.

[28] Schulz, R. B., Plantz, V. C., and Brush, D. R., "Shielding Theory and Practice," IEEE Transactions on Electromagnetic Compatibility, Vol.30, No.3, Aug. 1988, pp. 187—201.

[29] Zhou, J., et. al, "Measurements of thermal and dielectric properties of medium density fiberboard with different moisture contents," Bioresources, Vol.8, No. 3, 2013, pp.4185—4192.

[30] http://farr-research.com/